A Simple Method for Combining MCSST Data and In Situ Data in the Eastern Near-Equatorial Pacific

MICHAEL L. VAN WOERT*

SeaSpace, San Diego, California

(Manuscript received 24 January 1989, in final form 6 March 1990)

ABSTRACT

Ordinary least-squares is used to estimate the accuracy of monthly averaged sea surface temperature products in the eastern near-equatorial Pacific. Daytime multichannel sea surface temperature (MCSST) data, nighttime MCSST data, Climate Analysis Center (CAC) in situ temperatures, and CAC blended temperatures are all compared to monthly averaged, equatorial, 1 m moored-buoy temperatures at 110°W, 124°W, and 140°W. In addition, reduced least-squares (RLS) is used to develop regression equations between the CAC in. situ temperature and the MCSST data. Bootstrap methods are used to estimate the RLS regression statistics. These regression equations are used to convert the MCSST to equivalent in situ temperatures prior to combining the two datasets with a one over distance-squared gridding algorithm. Data used in this study are from the period January 1983 to December 1985. When data from the 1982/1983 El Niño are excluded from analysis, the MCSST data are not significantly different from the moored-buoy temperatures at the 5% significance level. The CAC in situ and blended temperatures have warm biases of 0.85°C and 0.70°C when compared to the moored-buoy temperatures. These differences are significantly different from zero at the 5% level. The bias between the daytime MCSST data and the CAC in situ data is 0.65°C when data from 1983 are excluded. The bias between the nighttime MCSST data and the CAC in situ data is 1.04°C. This difference is attributed to diurnal temperature fluctuations. The blended temperature product developed in this study is 0.94°C warmer than the moored-buoy temperature data. The shape of this blended product is similar to the CAC blend, but some differences exist. These differences are discussed.

1. Introduction

To produce the high quality, long-term, tropical sea surface temperature (SST) fields needed for climate studies, it will be necessary to supplement historical in situ data with current and future satellite data. Barnett et al. (1979) recognized the potential impact that remotely sensed, tropical SST data could have on global climate studies. They compared the NOAA global ocean sea surface temperature (GOSSTCOMP) product (Brower et al. 1976) to AXBT data collected as part of the Hawaii-to-Tahiti shuttle experiment (Patzert et al. 1978). They found that tropical GOSSTCOMP data were biased by 1°–4°C with respect to the AXBT observations. As a consequence of the large bias error, they concluded that GOSSTCOMP data were unsuitable for tropical climate studies.

In recent years remotely sensed SSTs have been available from an assortment of satellite sensors. To assess the accuracy of these different remotely sensed SST products, NASA/JPL sponsored three workshops to compare satellite-derived global SST products with in situ observations (Njoku 1985). Included in the workshop comparisons were multichannel sea surface temperature (MCSST) data, which are derived from algorithms that have replaced the GOSSTCOMP algorithm. The main conclusions of the workshops were first, that MCSST data are the most accurate remotely sensed global SST data available and second, that large temporally and spatially varying errors exist in the MCSST data (Bernstein and Chelton 1985). The JPL workshops did not provide regional comparisons of the SST products, but the work of Barnett et al. (1979) suggests that satellite-derived, tropical SST products should be carefully evaluated before they are used in climate studies.

In an effort to minimize the effects of errors in the MCSST data, the Climate Analysis Center (CAC) blends the MCSST data and the CAC in situ analysis by using the MCSST analysis to define the shape of the SST field and by using a heavily smoothed in situ analysis as the boundary conditions to the solution of Poisson's equation (Reynolds 1988). The CAC blended product is designed to filter out spatial features smaller than 6° of latitude or longitude. In the tropical Pacific, near 150°W, the dominant feature, the equatorial cold tongue, is approximately 6 degrees wide in the merid-

* Affiliation: Center for Hydrological Optics and Remote Sensing, San Diego State University, San Diego, California.

Corresponding author address: Dr. Michael L. Van Woert, 3655 Nobel Drive, Suite 160, San Diego, CA 92122.

ional direction (Fig. 1). Thus, to derive a blended product capable of fully resolving tropical SST variability, additional work is required.

This paper first assesses whether errors in the near-equatorial MCSST data and CAC in situ data are consistent with global error estimates derived from the JPL workshop analysis. Four monthly averaged, 2-degree latitude/longitude averaged, tropical Pacific, SST products are available for evaluation. The products are, daytime and nighttime MCSST data (Van Woert 1988), CAC in situ SST data (Reynolds 1988), and CAC blended in situ/MCSST data (Reynolds 1988). The time period for each dataset is January 1983 to December 1985. Each of these four temperature products are compared to monthly averaged, 1 m moored-buoy temperature data (Halpern 1984). The high-quality moored-buoy temperature data are an ideal reference dataset because they were excluded from the preparation of both the CAC in situ analysis and the derivation of the MCSST coefficients. The comparisons are made using regression analysis assuming that errors in the moored-buoy temperatures are much smaller than errors in the other measurements.

This paper then provides a simple alternative method for blending MCSST and in situ data. This is done first by deriving regression equations between the in situ data and the MCSST data with a technique that accounts for errors in both the dependent and independent variables. These regression equations are then used to convert the MCSST data to equivalent in situ temperatures. Lastly, the data are weighted by their variance and blended with a one over distance-squared algorithm.

2. Data

a. Moored SST data

A mooring near 0, 110°W has been providing tropical Pacific current and temperature information since 1979. It has been maintained as part of the Eastern Pacific Ocean Climate Study (EPOCS), (NOAA 1985; Halpern 1984). Additional moorings were deployed near 0°, 95°W for the period July 1981 to April 1983; 0°, 124°W from April 1984 to October 1985; and 0°, 140°W starting in April 1983 and running through August 1985. Gaps in the 1 m moored temperature record exist (Fig. 2) and are mainly due to instrument failure. Discussion here will be limited to the moorings near 110°W, 124°W, and 140°W for the period January 1983 to December 1985 because these data are coincident in space and time with the available MCSST data.

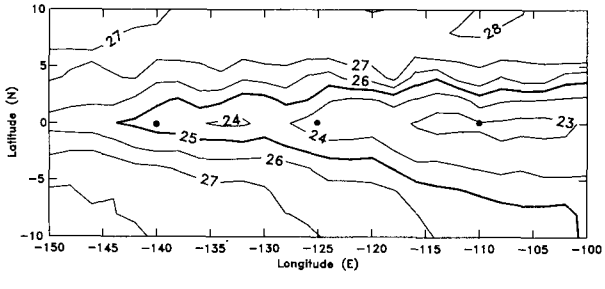

FIG. 1. Eastern tropical Pacific MCSST field for June 1984. Mooring locations at 110°W, 124°W and 140°W are denoted by (●).

The locations of the moorings are only nominal positions. For the period of interest the actual locations of the moorings deviate from these positions by as much as a degree of longitude, although mostly by not more than a few minutes of latitude and longitude. These variations in mooring position can produce discontinuities in the SST record if the moorings are moved within a region of strong SST gradients. Large discontinuities in temperature were not found in the data record at times when the moorings were set and recovered. Thus, for the monthly averaged data used in this study, the errors associated with the small variations in mooring locations should be small.

Monthly averaged SST at the mooring locations is of interest in this study. The raw moored temperatures actually represent 15 minute averages from a depth of 0.8–1.0 m. Their accuracy is reported to be 0.02°C based on precruise and postcruise calibrations (Halpern 1984). From these high-quality, 15 minute averages, monthly averaged SSTs were computed in three ways. First, a monthly average was formed by averaging all of the 15 minute observations within the month. Throughout the rest of this paper these will be referred to as monthly averaged, moored temperatures. Second, monthly averages were produced by averaging all of the 15 minute SST values for the month that had a local time between 0200 to 0300 LST. These will be referred to as monthly averaged, moored-nighttime temperatures. Third, monthly averages were computed from all of the 15 minute SST values within the month that had a local time between 1400 to 1500 LST. These will be referred to as monthly averaged, moored-daytime temperatures. The daytime and nighttime averaging periods were chosen because they approximate the time of day when the satellites (NOAA-7 and NOAA-9) pass over the moorings. This was done to minimize the effects of potentially large diurnal fluctuations on the comparisons. The three, monthly averaged moored temperature time series for each mooring are shown in Fig. 2.

b. MCSST data

The MCSST measurements are based on radiance measurements from the Advanced Very High Resolution Radiometer (AVHRR) sensor carried aboard the NOAA polar orbiting satellites. These radiances are collected by ground stations and then post processed to produce the MCSST estimates. A detailed description of the methodology for producing MCSST observations is given by McClain et al. (1985). Also, a brief description of the processing is provided here.

Starting with the launch of NOAA-7 in August 1981,

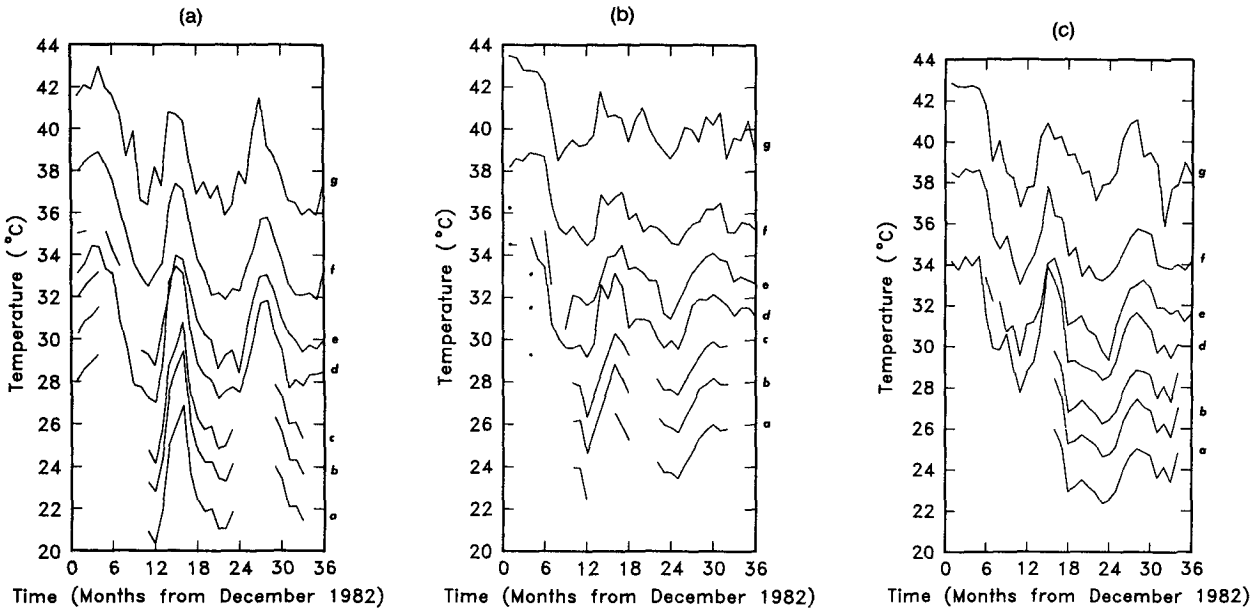

FIG. 2. (a) Three-year record of monthly averaged (*a*) moored, (*b*) daytime moored, (*c*) nighttime moored, (*d*) daytime MCSST, (*e*) nighttime MCSST, (*f*) CAC blend, and (*g*) CAC in situ temperature at 110°W. With the exception of the in situ series, which is offset from the preceding series by 4°C, all series are offset by 2°C. (b). Same as (a) except at 124°W. (c) Same as (a) except at 140°W.

NOAA has been operating satellites equipped with a five-channel AVHRR. The five channels correspond to a visible (0.58–0.68 μm), reflected infrared (0.725–1.1 μm) and three emitted infrared channels (3.55–3.93, 10.3–11.3, and 11.5–12.5 μm). The spatial resolution of the AVHRR is 1.1 km at nadir. These 1.1 km resolution data are referred to as Local Area Coverage (LAC) data. The satellite also produces subsampled LAC data called Global Area Coverage (GAC) data. GAC data are obtained from LAC data by averaging four of every five samples along a scan line from every third scan line. The resulting GAC data have about 4 km resolution.

These five channel GAC data form the starting point for the generation of the MCSST observations. The first step in the MCSST algorithm is to eliminate GAC samples contaminated by clouds and direct specular reflection. The specular reflection test is a geometrical test based on satellite and solar viewing angles. The cloud screening tests fall into three classes: visible or IR reflectance, uniformity, and channel intercomparisons. GAC data passing all of the tests are corrected for atmospheric attenuation using a linear combination of the IR channels and then are spatially averaged to produce MCSSTs. The resulting MCSST data have an 8 km square footprint, a nominal separation of 25 km in midocean, and a stated precision of 0.5°C when compared against high quality drifting buoys (Strong and McClain 1984). It is these raw data that are archived on the 7-day MCSST data tapes by the National Environmental Satellite Data and Information Services (NESDIS). These data form the starting point for the analysis discussed here.

The details of the MCSST data extraction and processing can be found in Van Woert (1988). Briefly, the data from the region 10°S–10°N, 100°–150°W were extracted from the 7-day MCSST tapes using information contained in the NOAA Polar Orbiter Data Users Guide (Kidwell 1986). These data were sorted in space and time into monthly, 2 degree latitude/longitude bins centered on even values of latitude and longitude. For each bin, or grid node, a monthly mean MCSST value, a monthly MCSST variance and the number of MCSST observations used in each grid node calculation were accumulated. Daytime and nighttime MCSST were processed separately to avoid potential problems resulting from differences in the daytime and nighttime MCSST algorithms and to prevent contaminating the comparisons with potentially strong diurnal variations. Monthly MCSSTs at the mooring locations were obtained by linearly interpolating between the two nearest equatorial grid values. During several months it was not possible to obtain a monthly averaged MCSST estimate because one or both of the adjoining grid nodes were undefined. These months were disregarded from further analysis. The two monthly averaged MCSST temperature time series at each mooring are shown in Fig. 2.

c. In situ data

The U.S. National Meteorological Center collects in situ SST data in near real time and then processes these

data to produce global maps of monthly averaged SST. These data include all drift buoy temperatures and routine ship observations (mostly ship injection temperatures). The production of the monthly maps includes the elimination of questionable data, averaging the data in 2-degree latitude/longitude bins, and then applying a nonlinear median filter. These data are adequate to describe the SST field between 30°S and 60°N except in the central and eastern tropical Pacific (Reynolds 1988). The monthly averaged in situ temperature time series at each mooring are shown in Fig. 2.

d. MCSST/in situ blended SST data

The MCSST and in situ gridded products are blended using a sophisticated algorithm that involves the solution of Poisson's equation on a sphere (Reynolds 1988). By including the MCSST analysis, this blended product overcomes the limitation of poor in situ data coverage in the tropical Pacific while retaining the structure of the in situ SST field in areas where in situ SST data are plentiful. For completeness, the blended product will be compared against the moored SST data, but it will not be compared against either

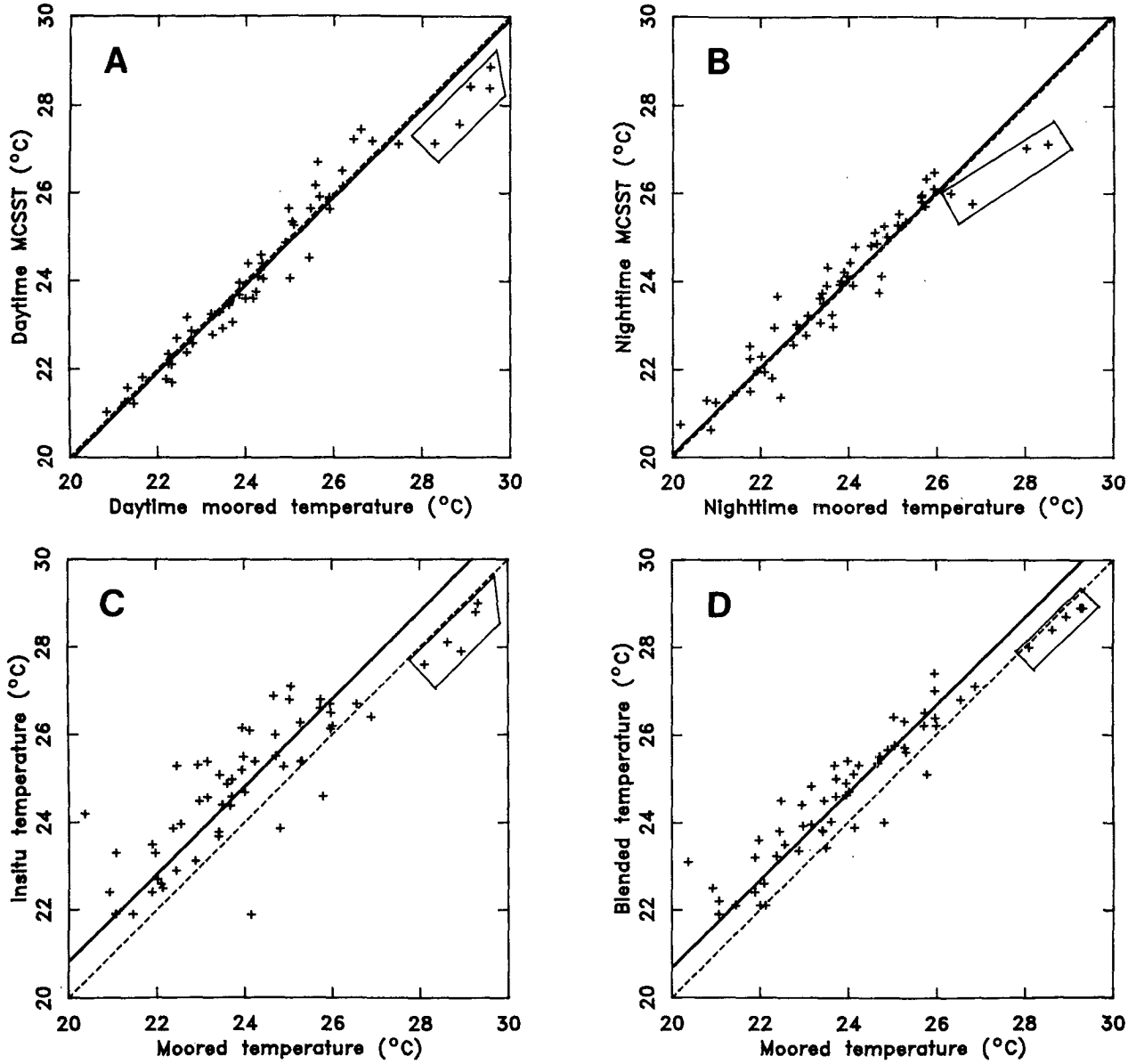

FIG. 3. Scatter plots and regression lines for (a) daytime MCSST data versus daytime moored temperature, (b) nighttime MCSST data versus nighttime moored temperature, (c) CAC in situ versus moored temperature and (d) CAC blend versus moored temperature. The solid line represents the regression model OTHER_SST = a_0MOOR_SST + b_0. The dashed line is the perfect-fit line. The data enclosed in the box are data from 1983, the period contaminated by El Chichón aerosols.

the in situ or MCSST data because the blended data are not statistically independent of the in situ and MCSST data. The monthly averaged blended temperature time series at each mooring is shown in Fig. 2.

3. Method

a. Ordinary least-squares

Residuals about regression lines between the four SST data products and the moored-buoy temperature data are used to estimate the errors in the daytime MCSST, nighttime MCSST, in situ SST, and blended SST products. Scatter plots of the data and the ordinary-least-squares (OLS) lines are shown in Figs. 3 and 4. The independent variable (abscissa) refers to one of the three monthly averaged moored datasets (MOOR_SST). The dependent variable (ordinate) refers to either the daytime MCSST data, the nighttime MCSST data, the in situ data, or the blended data (OTHER_SST). The specific data pairings are noted in the axis labels.

Two models were fit to the data. The first model is

$$\text{OTHER\_SST} = a_0\text{MOOR\_SST} + b_0, \quad (1)$$

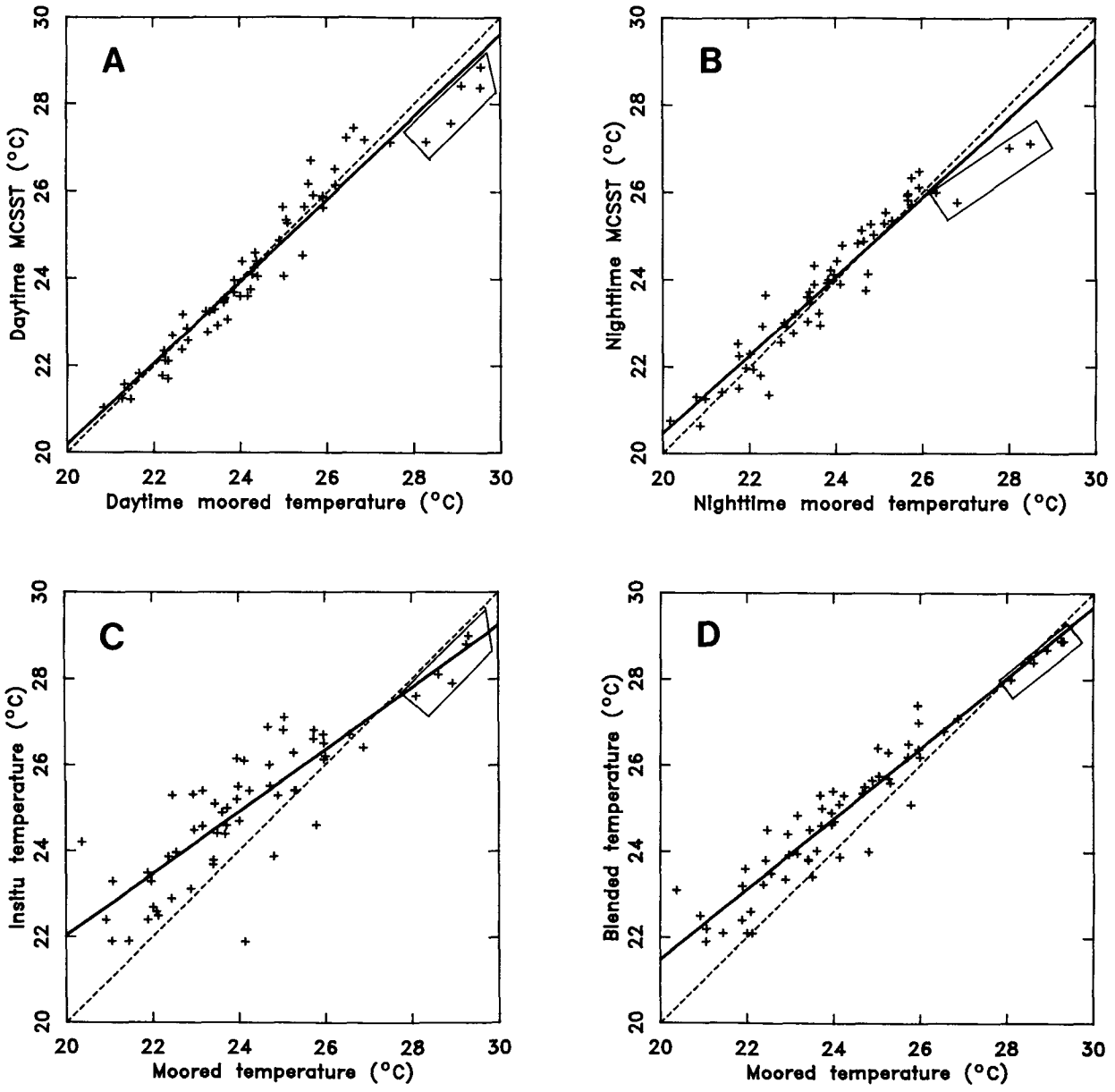

FIG. 4. Same as Fig. 3 except that the model plotted is OTHER_SST = a_1MOOR_SST + b_1.

TABLE 1. Regression statistics for the ordinary least-squares lines shown in Figs. 3 and 4.

		Bias model				Linear model								
Abscissa	Ordinate	b_0	95%	σ	χ^2	b_1	95%	a_1	95%	σ	χ^2	F	R	N
Daytime moored temp.	Daytime MCSST	−0.09	±0.12	0.49	54.52	1.31	±1.44	0.94	±0.06	0.47	51.24	3.59	0.97	59
Nighttime moored temp.	Nighttime MCSST	0.08	±0.13	0.52	58.56	2.33	±1.74	0.91	±0.07	0.49	52.28	6.34	0.96	56
Moored temp.	In situ temp.	0.84	±0.27	1.06	53.31	7.60	±2.71	0.72	±0.11	0.89	37.03	24.61	0.86	59
Moored temp.	Blended temp.	0.70	±0.17	0.68	41.38	5.12	±1.69	0.82	±0.07	0.56	28.27	25.98	0.95	59

where $a_0 \equiv 1$. Hereafter, this model is referred to as the bias model. The solid lines in Fig. 3 represent this model and the intercept with the ordinate axis (b_0) represents the temperature bias between the two datasets.

The second model relating the dependent datasets to the moored temperature data is

$$\text{OTHER\_SST} = a_1\text{MOOR\_SST} + b_1. \quad (2)$$

Hereafter, this model is referred to as the linear model. The solid lines in Fig. 4 represent this model.

For a least-squares fit to be useful it should provide estimates of the parameters, the uncertainty in the parameters, and an estimate of the goodness-of-fit (Press et al. 1986). In addition, in this study an estimate of the data uncertainty also is desired. The remainder of this section outlines how these quantities were estimated for the two models described above.

The coefficients b_0, b_1, and a_1 are estimated by minimizing chi-square, χ^2, which is defined as

$$\chi_k^2 = \sum_{i=1}^{N} \frac{(\text{OTHER\_SST}(i) - a_k\text{MOOR\_SST}(i) - b_k)^2}{\sigma^2} \qquad k = 0, 1. \quad (3)$$

Here N is the number of data pairs and σ is the standard deviation of an individual measurement. Estimates of σ are obtained by assuming σ is a constant, minimizing χ^2, and then solving

$$\sigma_k^2 = \sum_{i=1}^{N} (\text{OTHER\_SST}(i) - a_k\text{MOOR\_SST}(i) - b_k)^2/N \qquad k = 0, 1 \quad (4)$$

for σ.

Here, χ^2 and σ cannot be independently estimated because they are related to each other through Eq. (3). Global temperature statistics are expected to differ from the tropical values because of differences in the ocean structure, differences in the intervening atmosphere, and data sparsity. Therefore, global estimates will be used as the best available independent estimates of σ in the estimation of χ^2. The global error estimates used are 0.5°C for the MCSST data (McClain et al. 1985), 1.1°C for the in situ data (Reynolds 1988), and 0.8°C for the blended data (Reynolds 1988). The χ^2 values are listed in Tables 1 and 2.

The validity of the OLS method rests on the assumption that errors in the independent variable are much smaller than the errors in the dependent variable (E dependent $\ll E$ independent). This assumption is equivalent to assuming that 1 m moored temperatures are known perfectly and the other SST observations are in error; the assumption is probably valid. Each individual 15 min moored temperature measurement has a reported error of 0.02°C (Halpern 1984) and monthly averaged moored temperature errors should be even smaller. These are smaller than the global error estimates for all SST products listed above, and as will be shown later, they are also smaller than the errors in

TABLE 2. Same as Table 1 except data from the El Nino period have been excluded from the regression analysis.

		Bias model				Linear model								
Abscissa	Ordinate	b_0	95%	σ	χ^2	b_1	95%	a_1	95%	σ	χ^2	F	R	N
Daytime moored temp.	Daytime MCSST	−0.01	±0.11	0.41	32.45	−1.98	±1.76	1.08	±0.07	0.40	29.40	4.78	0.97	49
Nighttime moored temp.	Nighttime MCSST	0.08	±0.12	0.44	37.90	0.16	±2.00	1.00	±0.08	0.45	37.88	0.01	0.96	49
Moored temp.	In situ temp.	0.85	±0.26	0.92	40.32	5.26	±3.94	0.82	±0.16	0.88	36.56	4.73	0.82	49
Moored temp.	Blended temp.	0.70	±0.15	0.55	22.61	2.88	±2.40	0.91	±0.10	0.54	21.17	3.12	0.93	49

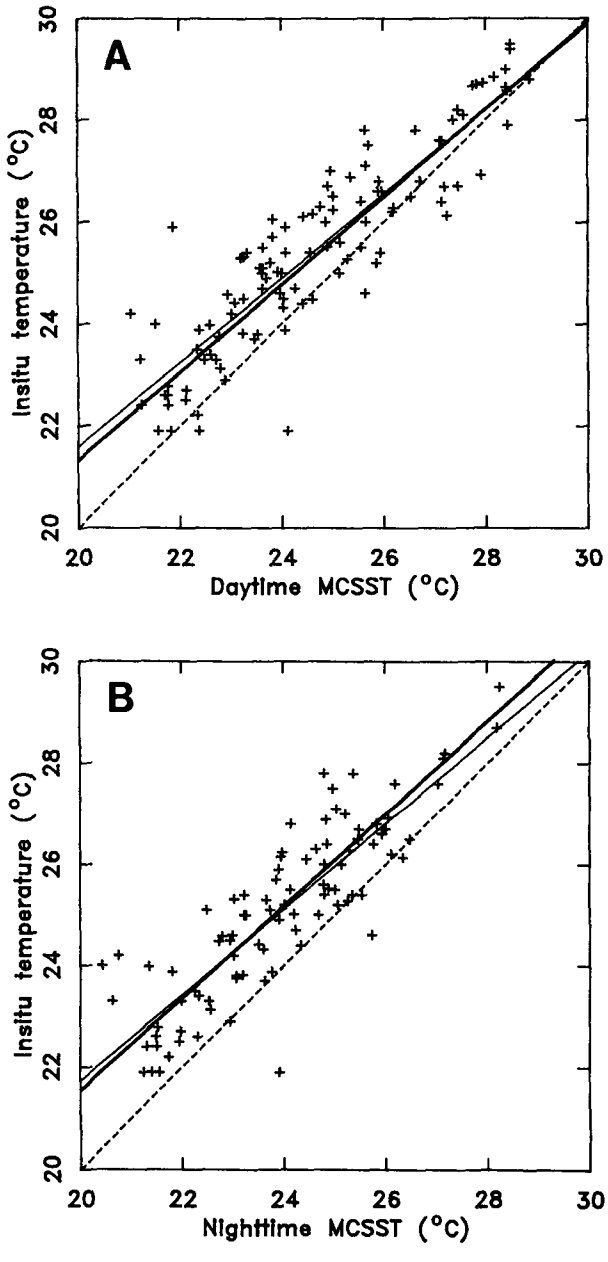

FIG. 5. Scatter plots and regression lines (a) CAC in situ temperature versus daytime MCSST, and (b) CAC in situ temperature versus nighttime MCSST. The thin line is the OLS line and the bold line is the RLS line. The dashed line is the perfect-fit line.

the tropical SST products. Thus, it should be possible to estimate b_0, b_1, and a_1 using OLS methods.

The minimum χ^2 is an estimate of the goodness-of-fit. In the limit of large N, a chi-squared distribution approaches a normal distribution with a mean equal to the number of degrees of freedom, $\nu = N - 3$, and a standard deviation equal to $\sqrt{2\nu}$. A fit is usually deemed a good fit if the computed χ^2 is approximately equal to the mean of a χ^2 distribution with ν degrees of freedom (Press et al. 1986).

Having determined the bias and linear regression statistics, an F-test is used to determine whether the linear model is significantly better than the bias model. For approximately 60 degrees of freedom the tabulated 5% level of significance, $F_{0.05}$, is 4.00 (e.g., Bevington 1969). If the computed F exceeds $F_{0.05}$, a_1 is probably nonzero and the linear term should be included; b_0, b_1, a_1, χ^2, and F are all listed in Tables 1 and 2.

b. *Reduced least-squares*

Until the recent operational implementation of the MCSST algorithm, in situ data were the only source of global SST data. It is well known that differences exist between MCSST data and in situ data (Bernstein and Chelton 1985). Further evidence of these differences is provided in this paper. To merge the MCSST data with the historical in situ data in a rational way, some form of calibration between the two datasets must be established. To achieve this, regression equations between the MCSST and in situ temperature were developed. Both bias and linear models, similar to Eqs. (1) and (2), were fit between the MCSST and in situ data.

Ordinary least-squares is valid only when the errors in the independent variable are much smaller than the errors in the dependent variable. It will be shown later that the assumption E dependent $\ll E$ independent is violated for tropical MCSST and in situ data. However, regression techniques have been developed to handle situations where both dependent and independent data have significant errors. These methods are referred to as reduced least-squares algorithms (RLS) (York 1966; O'Neill et al. 1969; Barker and Diana 1974). For comparison purposes both the RLS and the OLS lines are shown in Fig. 5.

c. *Bootstrap statistics*

Asymptotic expressions do not exist for estimating RLS parameter uncertainties. To estimate the RLS coefficient uncertainties a Monte-Carlo technique called bootstrapping (Efron 1979a, 1979b) was utilized.

Koblinsky was the first to apply bootstrap techniques to oceanographic data analysis (Koblinsky et al. 1984). The chief advantage of the bootstrap technique is that the results are usually insensitive to the data distribution. This makes it particularly attractive for estimating statistics of small samples that have poorly known data distributions.

The bootstrap method is relatively straightforward to implement, but it can put heavy demands on computer resources if the problem is complex. The details of the bootstrap method can be found in Efron (1979a, 1979b) and the application of the technique to least squares problems is provided by Freedman and Peters (1983). The method briefly stated is to define the parameters to bootstrap (in this case b_0, b_1, and a_1). Select

at random, N data values with replacement from the N original data points and compute the statistics. Repeat the process many times; for this work 1000 bootstrap samples were analyzed. The best estimate of each parameter is the median of the 1000 bootstrap estimates. The upper and lower 95% confidence limits were obtained from the upper and lower 2.5 percentile of the distribution. These were easily estimated by sorting the 1000 estimates and selecting the 25th, 500th, and 975th elements.

d. *Blending process*

Monthly blended MCSST/in situ maps for 1984 and 1985 were constructed for this study with a two-step blending algorithm. First, the gridded daytime and nighttime MCSST data were converted to equivalent in situ data using the bias adjustments given in Table 3b. Although linear regression equations were computed, they were not used in the blending process for reasons discussed in section 5f. Second, these calibrated MCSST maps (Figs. 6a, 6b, 7a, and 7b) along with the in situ maps (Figs. 6c and 7c) are combined in different ways depending on the data availability at each grid node. At grid nodes containing both MCSST and in situ data, blended grid node estimates were obtained by weighting the gridded SST estimates by their variance and then forming the average. For grid nodes that contain neither MCSST nor in situ data (this occurred rarely) an interpolated value was produced by averaging nearby MCSST and in situ gridded data that were weighted by their variance and one over distance-squared. Hereafter, this product is referred to as the least-squares blended product (LSQRBP).

4. Results

a. *Bias model*

Figure 3 displays the bias model regression lines between the moored temperature data and the other SST data. Table 1 lists the regression coefficients and statistics.

The daytime MCSST data relative to the daytime moored data, and the nighttime MCSST data relative to the nighttime moored data have small biases (−0.09°C, +0.08°C) that are not significantly different from zero at the 5% significance level. In addition, the correlation coefficients, R, exceed 0.95 indicating that the structure of the MCSST data is similar to the structure of the moored temperature data. The standard errors, σ, for both regressions are ~0.5°C.

In contrast, the in situ data and the CAC blended data are biased warm by 0.84°C and 0.70°C, respectively, relative to the moored temperature data. These biases are significantly different from zero at the 5% significance level.

b. *Linear model*

Figure 4 displays the linear regression lines and Table 1 lists the regression coefficients and statistics.

For the daytime MCSST data versus the moored temperature comparison, the slope and intercept are 0.94 and 1.31, respectively. These are not significantly different from 1.0 and 0.0, respectively, at the 5% significance level.

The nighttime MCSST data versus the moored temperature regression equation has an intercept that is significantly different from 0.0 and a slope that is significantly less than 1.0 at the 5% significance level. It should be noted, however, that the nighttime results are very similar to the daytime results (See also section 4e). Thus, the statistical results for the nighttime regression may not be valid.

The remaining two regressions, in situ temperature and blended temperature versus moored temperature, both have positive intercepts that are significantly different from 0.0 and slopes that are significantly less than 1.0 at the 5% significance level.

These lines represent clockwise rotations of the unit slope lines in Fig. 3. The rotated lines indicate that at warmer temperatures (near 30°C) the SST products are cooler than the moored temperatures. At cooler temperatures (near 20°C) the SST products are warmer than the moored temperature. The linear model produces a substantial reduction in the standard error when compared to the bias model.

c. *Bootstrap parameter uncertainties*

It was unnecessary to bootstrap the OLS regression equations; however, bootstrapping was applied to the OLS regressions to validate the bootstrap method. Some small, insignificant differences were noted.

Specifically, the results (not shown) of bootstrapping the bias, b_0, indicate that the median bootstrap values differ from the original data estimates by several hundredths of a degree Celsius. This difference is thought to be an artifact of the bootstrap technique (Efron 1979b). The spread between the bootstrapped 5% significance limits, however, are identical to the asymptotic limits (Table 1) obtained when the data errors are assumed to be normally distributed.

Here, b_1 and a_1 in the linear model were also bootstrapped. The median bootstrap values of the intercepts, b_1, are slightly smaller than the original estimates of the intercept. The slopes, a_1, are either unchanged or just slightly larger (closer to 1.0) than the original slopes. The bootstrap confidence limits are consistent with the asymptotic limits (Table 1) obtained when the data are assumed to be normally distributed.

All of the differences between the bootstrap technique and asymptotic limits are small, which provides some justification for using bootstrap techniques to estimate uncertainties in the RLS coefficients.

d. Goodness-of-fit

Chi-squared values are listed in Table 1. The nighttime bias model regression has the largest χ^2 (58.6) and the blended bias model has the smallest χ^2 (41.4). All are close to N ($\sim$60), which indicates that all are reasonably good fits. As expected, the linear model χ^2 values are slightly smaller than the bias model values.

e. Significance of linear model

An F-test was used to determine whether the linear model is significantly better than the bias model. For approximately 60 degrees of freedom the tabulated F-value is 4.00 (e.g., Bevington 1969). The computed F-values for the regressions are provided in Table 1. The F-values for the daytime and nighttime regressions are close to 4.00; thus, the linear terms are probably unimportant. The F-values for the in situ and blended regressions, however, are much larger than 4.0. In these cases the linear terms definitely are important, thus, indicating a temperature dependent bias between the CAC in situ/blended products and the moored-buoy temperature.

f. Least squares excluding data from 1983

A common misuse of the OLS technique is to apply the method without careful consideration of the data distribution. Outliers, or more appropriately points with a very low probability of occurrence based on a Gaussian error distribution, can corrupt OLS solutions because the maximum likelihood estimator is willing to distort the model parameters to bring them, mistakenly, into line with the outlying data. To be assured that the results are not sensitive to the values of individual data points it is necessary to eliminate outliers and reanalyze the data. If the results remain unchanged usually it can be assumed that the results are insensitive to the outlying values.

It is well documented that MCSST data from 1982 and early 1983 were strongly affected by aerosols produced during the eruption of the Mexican volcano, El Chichon (Strong 1986). Radiometric temperatures affected by aerosols normally appear anomalously cool with respect to the true temperature. Apparent outlying data collected during this period are enclosed in boxes in Figs. 3 and 4. The regression statistics excluding these data (and several other values that could not be boxed) are listed in Table 2.

Deletion of the anomalously cool MCSST data from 1983 produced a small warm bias in all temperature products relative to the moored-buoy data. The linear model produced smaller intercepts and slopes closer to 1.0 when data from 1983 were excluded.

Exclusion of the data from 1983 dramatically reduced all of the F-values except the value for the daytime regression, which increased slightly. In all cases the F-values are close to 4.00; thus, the linear terms are probably unnecessary in any of the regressions against the moored-buoy data.

g. Regression of MCSST data against in situ data

The results of the RLS bias model regression (Table 4a) indicate that the daytime MCSST data are approximately 0.8°C cooler than the in situ data and the nighttime MCSST data are 1.1°C cooler than in situ temperatures. Both coefficients are significantly different from zero at the 5% significance level. The daytime and nighttime monthly averaged MCSST data also are significantly different from each other at the 5% significance level. This result is independent of whether the data are assumed to be statistically paired or unpaired.

The RLS slope and intercept for the linear model relating the daytime MCSST and in situ temperature are 0.86°C and 4.11°C. The slope is significantly different from 1.0 and the bias is significantly different from 0.0, both at the 5% significance level. The F-value indicates that the linear term is significant. The RLS slope and intercept between the nighttime MCSST data and the in situ temperature are 0.9°C and 3.32°C. The slope is not significantly different from 1.0 and the intercept is not significantly different from 0.0, both at the 5% significance level. The F-value indicates that the linear term is unnecessary.

Regressions were also run between the MCSST data and in situ data excluding data from 1983. Exclusion of these data altered the regression coefficients and statistics (Table 4b), but the regression lines (not shown) looked similar to those in Fig. 5 and the results remain unchanged.

h. Blending MCSST and in situ

Figures 6 and 7 show the daytime MCSST, nighttime MCSST, CAC in situ temperature, CAC blended temperature, LSQRBP temperature, and the LSQRBP-CAC blended temperature difference for November 1984 and March 1985. November 1984 was chosen for discussion because it is a month when the equatorial cold tongue was well developed. March 1985 was chosen because it is a month when the cold tongue was absent.

As noted by the location of the 25°C isotherm, the CAC blended product (Fig. 6d) looks similar to the in situ map (Fig. 6c) and the LSQRBP (Fig. 6e) closely resembles the MCSST maps (Figs. 6a and 6b). Overall, however, the differences between the two blended products (Fig. 6f) do not exceed ±0.5°C.

The March 1988 maps present a slightly different situation. This time the CAC blend (Fig. 7d) looks very similar to the nighttime MCSST field (Fig. 7b). The shape of the LSQRBP field (Fig. 7e), however,

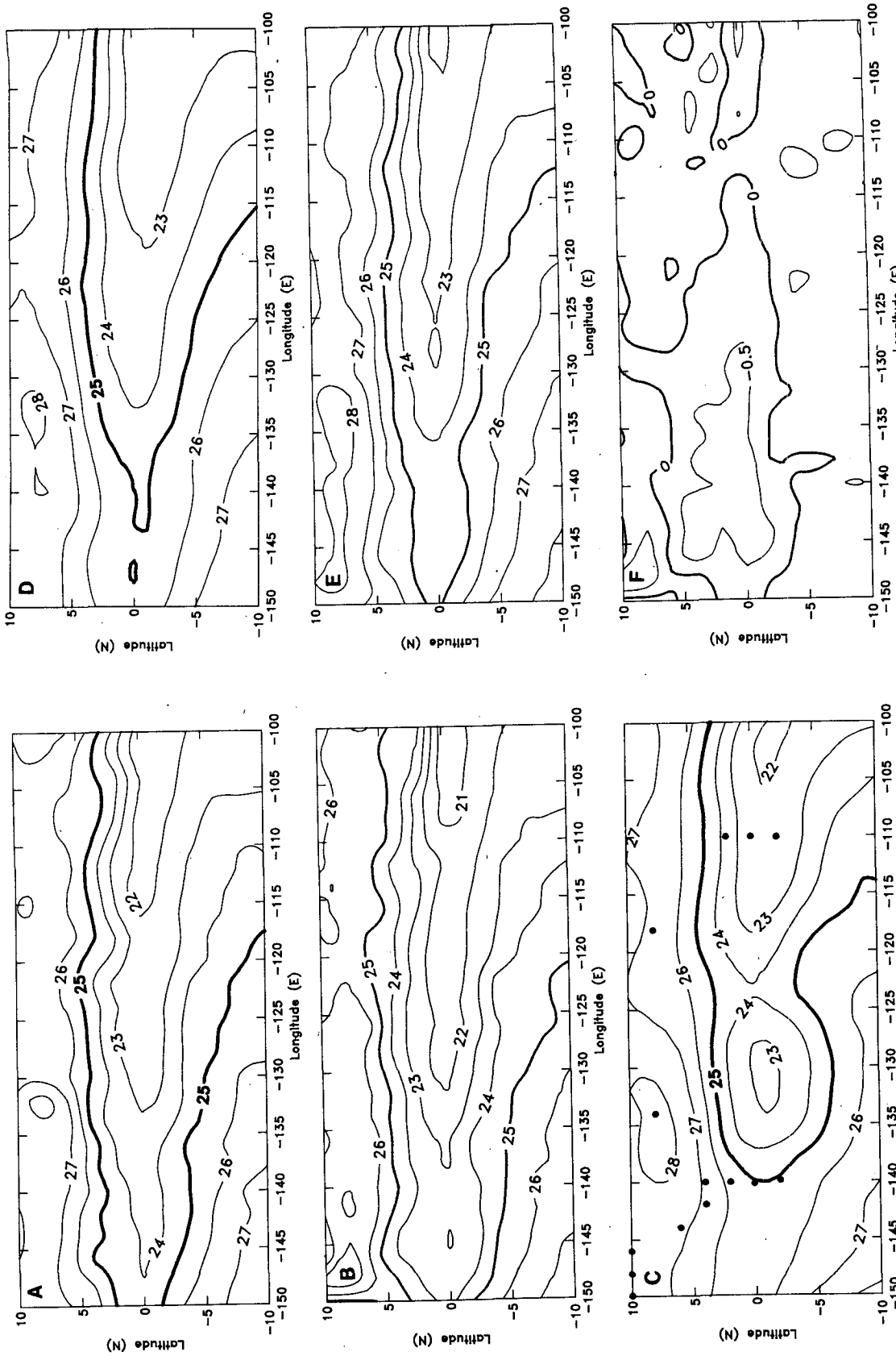

FIG. 6. Monthly averaged, eastern tropical Pacific SST maps for November 1984. The maps represent (a) daytime MCSST, (b) nighttime MCSST, (c) CAC in situ temperature, (d) CAC blended temperature, (e) LSQRBP temperature and (f) LSQRBP–CAC blend temperature difference. The (●) in Fig. 7c indicate grid nodes that were estimated from 5 or more in situ reports during the month.

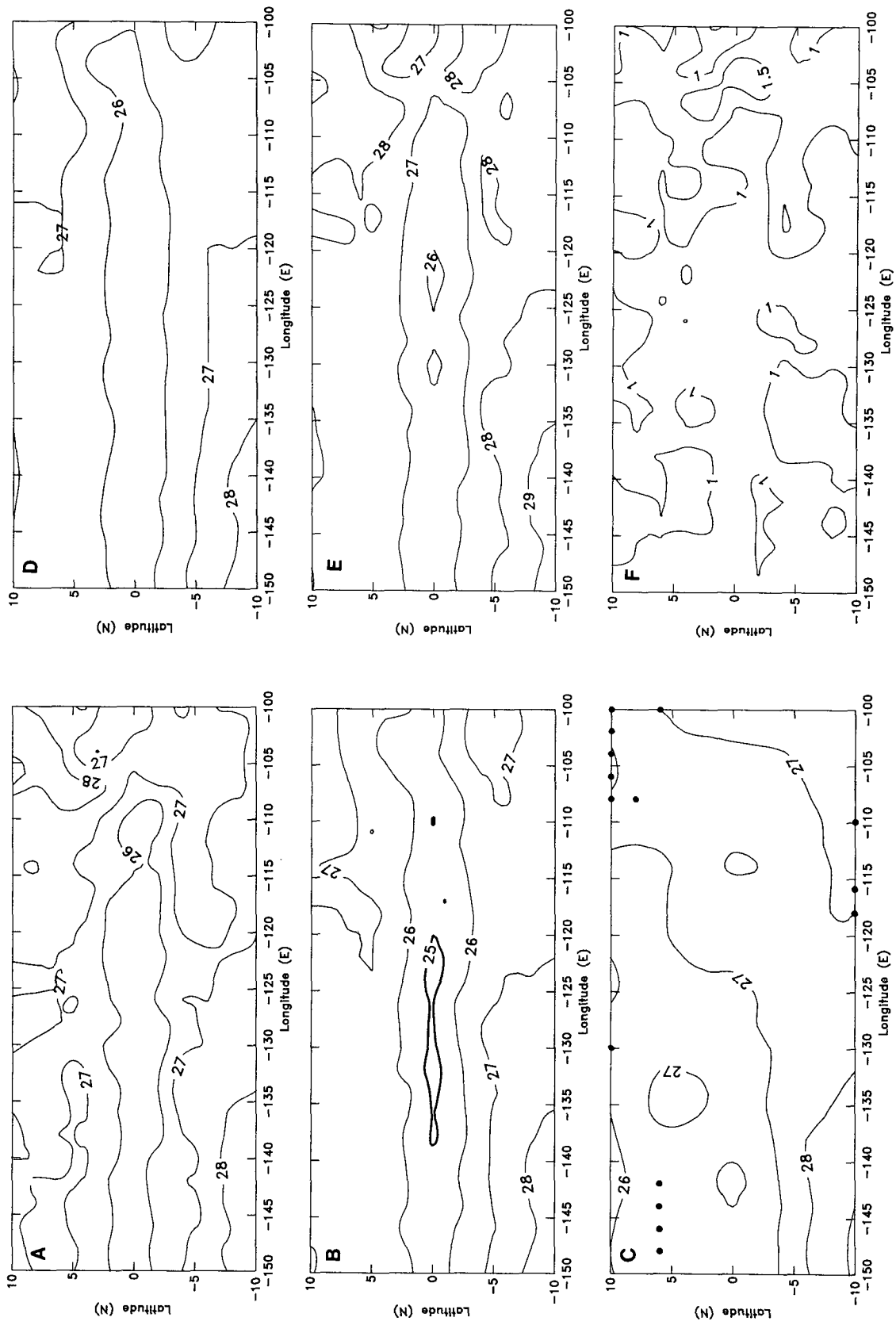

FIG. 7. Monthly averaged, eastern tropical Pacific SST maps for March 1985. The maps represent (a) daytime MCSST, (b) nighttime MCSST, (c) CAC in situ temperature, (d) CAC blended temperature, (e) LSQRBP temperature and (f) LSQRBP–CAC blend temperature difference. The (●) in Fig. 8c indicate grid nodes that were estimated from five or more in situ reports during the month.

more closely resembles the shape of the daytime MCSST map (Fig. 7a). Neither resembles the in situ analysis. The difference field (Fig. 7f) indicates that the LSQRBP is warmer than the CAC blend by about 1°C except along the equator near 105 degrees W. There the difference exceeds 1.5°C. This 1.5°C anomaly occurs because the CAC blend appears to be dominated by the nighttime MCSST, which does not include the warm anomaly seen near 105°W in the daytime MCSST product.

The LSQRBP data were compared to the moored-buoy data. A warm bias of 0.74°C exists between the LSQRBP and the moored-buoy temperatures, which is significantly different from 0.0 at the 5% significance level. The standard error is 0.57°C, the correlation coefficient is 0.95°, and the χ^2 is 25.6. The linear term is deemed unnecessary based on the results of an *F*-test when data from 1983 were excluded from the analysis.

5. Discussion

a. MCSST errors

The MCSST algorithm is tuned against a global set of drifting buoys that report temperature from a nominal depth of 1 m (McClain et al. 1985). The MCSST algorithm, therefore, is not designed to provide estimates of the skin temperature. Rather, the MCSST algorithm uses observed radiometric temperatures and globally derived MCSST regression coefficients to produce temperatures extrapolated to 1 m.

Several studies have used drift-buoy data to verify the MCSST algorithms, (Bernstein 1982; McClain et al. 1985; Strong and McClain 1984), but Strong and McClain provide the only comparison between MCSST data and moored-buoy temperatures. They found that MCSST data had a cool bias with respect to the moored-buoy temperatures (moored-buoy temperature–MCSST) of 0.47°C and a root mean square difference (RMSD) of 1.05°C. They attributed the large RMSD to the large SST gradients characteristic of coastal regions where most of the moored buoys are anchored and the lack of space/time coincidence between the data. However, other factors such as diurnal fluctuations, caused by the inclusion of both nighttime and daytime MCSST data in the comparison, and the failure to remove the 0.47°C bias prior to computing the RMSD could contribute to the large observed RMSD.

To minimize these problems they carefully rederived the MCSST coefficients using a global set of drifting buoys. The rederived MCSST data were then compared against an independent set of drift-buoy data. They were not recompared to moored-buoy data, but both the nighttime and daytime comparisons against the drift-buoy temperatures produced biases of approximately −0.02°C and RMSDs of ~0.5°C. These global statistics are consistent with the tropical MCSST verses moored-buoy temperature statistics presented in this study (Tables 1–2).

Nonstationary events such as the launch of new satellites also can lead to errors in the MCSST data. Reynolds et al. (1989) found daytime MCSST errors of 0.5–1.0°C in western tropical Pacific MCSST data. These errors occurred coincident with the launch of NOAA-11 in November 1988 and were probably due to an error in the implementation of the nonlinearity correction to the AVHRR calibration algorithm. February 1985 represented a transition from NOAA-7 MCSSTs to NOAA-9 MCSSTs. To investigate the effects of the satellite changeover on the tropical SST, each monthly averaged daytime MCSST map was zonally averaged and a contour plot of zonally averaged temperature versus latitude and time was produced (not shown). This map was smooth and continuous through the changeover from NOAA-7 to NOAA-9, thus a sensor-dependent error during the period, if present, was small.

b. In situ temperature errors

Historically, global SST maps have been based primarily on ship injection temperatures. Previous studies have shown that the injection temperatures at 5–10 m are biased warm with respect to high-quality surface temperatures. Saur (1963) found ship injection temperatures to be 0.6°C warmer than bucket temperatures. Barnett (1984) also compared bucket and injection temperatures and found a warm bias of 0.4°C. Tabatta (1978) reported a bias of 0.2°C between injection temperatures and temperatures at NOAA buoy stations. In this study the CAC in situ analysis was also found to be warmer than the moored-buoy temperatures, but this time it is warmer by 0.84°C (Table 1).

Three reasons have been suggested to explain this discrepancy. First, injection temperatures are usually measured in the ships engine room where heat from the ships engines can warm the water prior to the temperature reading. Second, bucket temperatures are likely to read anomalously cool due to evaporative heat losses if the bucket is not well insulated (Folland et al. 1984). Three, during periods of low wind speed, cool air, and warm surface water, evaporative cooling at the sea surface can produce differences between skin temperature and bulk temperature of 1°C or more (Katsaros 1980). Often, all three factors can contribute to the observed discrepancy.

One additional reason that has not been mentioned, is that improper sampling of near-equatorial in situ, blended, and MCSST temperatures can lead to an apparent bias when compared to the equatorial moored data. The eastern tropical Pacific is characterized by a strong north–south temperature gradient (Wyrtki and Kilonski 1984). The equatorial data products are formed from 2 degree spatial averages about the equator. Depending on the locations of the observations within the 2 degree box, the spatial average of the data

products can be as much as 0.5°C warmer than the temperature exactly on the equator. This is particularly true of the in situ product, which on occasion may rely on a single observation within the 2 degree box for the equatorial grid estimate.

c. *Discussion of MCSST versus in situ regression*

Bernstein and Chelton (1985) reported on the results of the JPL workshop SST comparisons. They found the in situ data to be 0.3°–0.5°C warmer than the MCSST product. This is smaller than the tropical biases (Table 3), which are 0.8°–1.1°C. Their reported standard errors also were slightly smaller, 0.5°–0.8°C, versus standard errors of 0.9°C for the RLS results described in this paper. The large differences found in this study between the equatorial CAC in situ temperatures and the MCSST data are probably due to the use of sparse, poor-quality, in situ observations to form spatial averages in a region of strong horizontal temperature gradient as discussed above.

Chelton (1985) and Bernstein and Chelton (1985) also used a three-way-error partitioning technique to estimate the RMSDs for three satellite-derived SST products. The method is similar to the more commonly used two-way-error partition method (e.g., Johnson et al. 1988). Essential to both methods is the assumption that the errors in each SST product are uncorrelated. While it is certainly true that the instrument noise of each sensor is independent, geophysical effects such as incomplete cloud filtering, SST dependent biases or diurnal fluctuations can render the method inappropriate. Despite these limitations Bernstein and Chelton found global RMSDs of 0.5°–0.7°C, which are consistent with their previous results.

Both two-way-error and three-way-error partitioning methods were applied to the data in Fig. 2. In this study, neither the two-way nor the three-way techniques produced acceptable results. For most choices of two or three datasets the RMSDs were unreasonably small and in some cases the RMSDs were actually negative. This is impossible unless one or more of the neglected cross correlation terms were important in the analysis. It has been shown that temperature-dependent biases may exist in the data. These can lead to nonzero correlations that can corrupt the two-way and three-way error estimates.

d. *Diurnal variations*

A second potential source of error in the two-way and three-way methods is incompletely resolved diurnal variability. Diurnal differences in the bulk temperature occur in the upper 10 m during periods of light winds and limited cloud cover. Pullen (1985) compared continuous underway temperatures from 5 m depth with hourly bucket temperatures in the tropical Pacific. On some days diurnal temperature differences of 1°–2°C were found. Furthermore, the mini-

TABLE 3. (a) Bootstrap estimates of regression statistics for the RLS bias and linear regression lines. The linear regression lines are shown in Fig. 5, (b) bootstrap estimates of regression statistics for the RLS regression lines excluding data from 1983.

		Bias model					Linear model							
Abscissa	Ordinate	−95%	b_0	+95%	σ	χ^2	−95%	b_1	+95%	a_1	+95%	σ	χ^2	F	R	N
a																
Daytime MCSST	In situ temp.	0.63	0.79	0.97	0.92	88.32	2.29	4.11	6.08	0.79	0.94	0.85	79.30	10.21	0.90	107
Nighttime MCSST	In situ temp.	0.94	1.11	1.31	0.91	74.18	0.78	3.32	6.17	0.79	1.01	0.87	70.74	2.77	0.86	93
b																
Daytime MCSST	In situ temp.	0.44	0.65	0.86	0.90	56.98	1.85	4.95	7.81	0.71	0.82	0.95	0.83	50.21	7.63	0.85	72
Nighttime MCSST	In situ temp.	0.83	1.04	1.27	0.94	59.33	−0.04	3.79	7.46	0.73	0.88	1.04	0.90	56.08	2.33	0.81	72

mum and maximum temperatures occurred at roughly the same times as the two daily satellite overpasses.

There is some evidence of diurnal variability in the MCSST data (Table 3b). The daytime MCSST data are 0.65°C cooler than the in situ data. At night the MCSST data are 1.04°C cooler than the in situ data. Since the same in situ data were used in both regressions, the 0.4°C difference observed between daytime and nighttime biases must be attributed to day/night differences in the MCSST data. Reynolds (1988) also noted day/night MCSST differences of 0.0°–0.5°C in the eastern tropical Pacific. These differences are now routinely monitored at the CAC (Reynolds et al. 1988).

e. Blending MCSST and in situ data: bias model

In this study an alternative to the CAC blended product is presented. Its main virtues are that it is easy to prepare because it does not require the solution of a partial differential equation and it provides better spatial resolution. Its main limitation is that it is based on regionally derived regression equations that may vary in space and time.

Overall, the difference, LSQRBP–CAC blend is larger in March 1985 than it is in November 1984 (Figs. 6f and 7f). One possible reason for the large difference observed during March is that during that month the equatorial cool tongue was not present. The cessation of the equatorial upwelling along with the strong solar heating (Gautier 1988; Gautier et al. 1986) can produce a strong vertical temperature gradient in the surface layer. During these periods the regression equations (Table 3) may not adequately relate the MCSST data extrapolated to 1 m and in situ temperature measured 10–15 m.

This does not imply that either the MCSST data or the in situ data are necessarily in error. Rather, it suggests that the assumed, time-invariant regression equations do not adequately characterize a possibly time-dependent relationship between the two datasets. This highlights the fundamental problem with all algorithms that blend in situ data and MCSSTs, that they attempt to combine two temperature measurements that are difficult to combine because they are related by complex physical processes. However, if the two measurements must be combined, the blending algorithm must account for temporal (and spatial) differences in the relationship between the MCSST field and the in situ field. The LSQRBP cannot attempt to model temporal differences, but the CAC blending technique can account for temporal differences at least in an ad hoc way.

In addition to potential time-dependent differences between the two blends, there is also some indication of spatial differences. For example, the November 1984 LSQRBP is cooler than the CAC blend on the equator, but the temperature difference reverses at about 5°N and 5°S (Fig. 6f).

Three reasons are offered to explain this difference. First, the difference could be the result of using equatorially derived regression equations in regions where they may not apply. To determine the validity of this explanation it will be necessary to compare each blended product with moored data north and south of the equator. These comparisons were not done in this study. Second, rapidly changing atmospheric conditions (in particular moisture and clouds) north and south of the equator can have a pronounced affect on the MCSST data and the subsequent blended products. This reason seems unlikely, however, because both blends depend strongly on the MCSST data in this region of the world, thus, negating much of the expected difference between the two blends. Third, the difference could be due to discrepancies in the CAC model. The CAC model uses the best ("best" being defined as >5 observations per grid node) in situ grid nodes as boundary conditions (anchor points). At locations distant from the anchor points, the solution is propagated into the interior with Poisson's equation. The solution to Poisson's equation is critically dependent on the boundary values. If the boundary conditions are in error these errors will be propagated into the interior region. To minimize the effects of these errors, the CAC in situ analysis is heavily smoothed. However, this leads to smoothing of the blended field, which could be responsible for the spatial differences observed between the two blends. Similar reasoning also could explain the differences between the March blended products.

f. Blending MCSST and in situ data: linear/bias model

It was shown (Table 3, Fig. 5) that the linear regression term is important for relating daytime MCSST data to in situ temperature, while a bias adjustment is sufficient to convert nighttime MCSST data to equivalent in situ data. Blended maps based on MCSST data that are scaled by these equations are not shown because the LSQRBP–CAC-blend maps usually have an east–west temperature trend (LSQRBP warmer than the CAC blend in the east and cooler than the CAC blend in the west). There are several potential reasons for this trend.

First, the eastern tropical Pacific is subject to spatially varying amounts of atmospheric aerosols that can produce depressions in the radiometric temperature. Smoke from slash burning in Central America has been noted in the eastern tropical Pacific during the spring prior to planting (Rao et al. 1989). Algorithms are under development to correct the daytime MCSST data for the effects of atmospheric aerosols (Rao et al. 1989; Durkee personal communication), but currently these algorithms have not been merged into the operational MCSST algorithm. It is unlikely, however, that aerosols are responsible for the observed temperature trend because both blends depend strongly on the MCSST data in the eastern near-equatorial Pacific.

A more likely reason for the east–west trend in the

LSQRBP–CAC-blended-difference maps is that the linear regression equation, which can be thought of as a temperature dependent bias correction, is inconsistent with the CAC blend. This point is easily illustrated by selecting a representative MCSST from the western edge (25°C) and a representative MCSST from the eastern edge (20°C). The CAC blend is 26°C in the west and 21°C in the east. Using the calibration coefficients from Table 3b, the 25°C MCSST converts to 25.5°C, which is 0.5°C cooler than the CAC blend. The 20°C blend converts to 21.4°C, which is 0.4°C warmer than the CAC blend. These differences are consistent with the observed trends in the difference field.

Three reasons were given in section 5e to explain the differences between the LSQRBP bias model blend and the CAC blend. These reasons may also explain some of the differences between the linear LSQRBP and the CAC blend. However, if the differences are due to errors in the LSQRBP, it implies that the derived linear regression equations do not properly account for spatial variations in the relationship between in situ temperature and MCSST data. The actual reason for the trend is unknown.

6. Conclusions

1) Excluding MCSST data from 1983, which are probably contaminated by El Chichon aerosols, the eastern near-equatorial Pacific, monthly averaged daytime and nighttime MCSST data have biases that are not significantly different from zero at the 95% confidence level when compared against coincident monthly averaged daytime and nighttime moored-buoy temperatures. The standard deviations for both the daytime and nighttime data are estimated to be ~0.5°C. Inclusion of a linear term is unnecessary in the nighttime regression and probably is unimportant in the daytime regression. In all cases monthly averaged MCSST data provide a good approximation to monthly averaged, 1 m, moored-buoy temperatures along the equator in the eastern Pacific.

2) Eastern near-equatorial Pacific, monthly averaged, CAC in situ temperatures are 0.8°C warmer than moored-buoy temperatures. The standard deviation for the in situ data is estimated to be ~1°C. Use of a linear regression equation rather than a simple bias adjustment is probably unnecessary.

3) Eastern near-equatorial Pacific, monthly averaged, CAC blended temperatures are 0.7°C warmer than the moored-buoy temperatures. The standard deviation for the CAC blended data is estimated to be ~0.7°C. Use of a linear regression equation rather than a simple bias adjustment is probably unnecessary.

4) Eastern near-equatorial Pacific, monthly averaged, CAC in situ temperatures are 0.8°C warmer than the daytime MCSST data and 1.1°C warmer than the nighttime MCSST data. The standard deviation for both regressions are ~0.9°C. Use of a linear regression equation rather than a simple bias adjustment significantly improves the fit between the daytime MCSST data and the CAC in situ data, but is unnecessary for the regression with the nighttime MCSST data.

5) Inclusion of the data from 1983 affected the MCSST versus moored-buoy temperature regression equations, but the effect was small compared to the impact the 1983 data had on the in situ and CAC blended regressions with the moored-temperature data. Atmospheric aerosols are expected to affect the MCSST data, but should not affect the in situ or CAC blended data. Therefore, the large differences in the regression coefficients must be due to noise in the in situ data and to differences in the physical processes relating temperature at 1 m with temperature at 10 m, not atmospheric aerosols.

6) A small (~0.4°C), but significantly nonzero, diurnal difference exists between the monthly averaged daytime and nighttime MCSST data in the eastern near-equatorial Pacific.

7) Nonstationary events such as the launch of a new satellite or aerosol outbreaks such as the one produced by the eruption of El Chichon may produce errors that are not immediately identified. Although the satellite data used in this study agreed favorably with the moored data, the accuracy of satellite data should always be carefully evaluated before use.

8) This paper presents the results of an attempt at blending MCSST and in situ data by converting gridded MCSST data to equivalent in situ temperatures. Potentially large temporal and spatial differences were observed between the CAC blended product and the LSQRBP developed here. While the LSQRBP may not be an improvement over the CAC blend, the exercise suggests that an upper ocean model probably should be used to relate MCSST data and in situ temperature rather than relying on regression equations or solutions to Poisson's equation. In addition, this study suggests that the CAC blending algorithm should be carefully examined to determine how errors in the anchor points propagate into the interior solution.

9) The analysis presented here indicates that at least along the equator the MCSST data compared better with the moored data than it did with either of the two blended products or the in situ data. Therefore, any errors in the blended products along the equator must be attributed to the degradation of the MCSST data by the in situ data.

10) More work is required to properly relate MCSST and in situ temperature. Once done, however, the individual MCSST and in situ observations can be blended using objective gridding techniques (Carter and Robinson 1987). The main advantage of an objectively gridded (or least-squares optimally interpolated) product is that error estimates of the temperature field also are produced, something that is currently unavailable for the CAC blended product.

Acknowledgments. The author thanks Richard Reynolds, Eric S. Johnson, and the reviewers for many useful comments. The in situ and blended data were provided by Richard Reynolds and the moored temperature data were provided by David Halpern. The use of these data is greatly appreciated. Thanks also to Evelyn Young for her help with the preparation of the figures and tables. Partial support for this study was provided by the National Science Foundation (contracts OCE-8314860 and OCE-8517377).

REFERENCES

Barker, D. R., and L. M. Diana, 1974: Simple method for fitting data when both variables have uncertainties. *Amer. J. Phys.*, **42**, 224–227.

Barnett, T. P., 1984: Long-term trends in sea surface temperature over the oceans. *Mon. Wea. Rev.*, **112**, 303–312.

——, W. C. Patzert, S. C. Webb and B. R. Bean, 1979: Climatological usefulness of satellite determined sea-surface temperatures in the tropical Pacific. *Bull. Amer. Met. Soc.*, **60**, 197–205.

Bernstein, R. L., 1982: Sea Surface temperature estimation using the NOAA 6 satellite advanced very high resolution radiometer. *J. Geophys. Res.*, **87**(C12), 9455–9465.

——, and D. B. Chelton, 1985: Large-scale sea surface temperature variability from satellite and shipboard measurements. *J. Geophys. Res.*, **90**(C6), 11 619–11 630.

Bevington, P. R., 1969: *Data Reduction and Error Analysis for the Physical Sciences.* McGraw Hill, 336 pp.

Brower, R. L., H. S. Gohrband, W. G. Pichel, T. L. Signore and C. C. Walton, 1976: Satellite derived sea surface temperature from NOAA spacecraft. NOAA Tech. Memo. NESS 78, U.S. Dept. of Commerce, Washington, DC, 74 pp.

Carter, E. F., and A. R. Robinson, 1987: Analysis models for the estimation of oceanic fields. *J. Atmos. Oceanic Technol.*, **4**, 49–74.

Chelton, D. B., 1983: Three-way partitioning of sea surface temperature measurement error. *Satellite-Derived Sea Surface Workshop—I,* JPL Publication 83-34, G1–G2 pp.

Efron, B., 1979a: Computers and the theory of statistics: Thinking the unthinkable. *SIAM Review,* **21**(4), 460–480.

——, 1979b: Bootstrap methods: Another look at the jackknife. *Annuls Stats.* 7(1), 1–26.

Folland, C. K., D. E. Parker and F. E. Kates, 1984: Worldwide marine temperature fluctuations 1856–1981. *Nature,* **310**, 670–673.

Freedman, D. A., and S. E. Peters, 1983: *Bootstrapping a Regression Equation: Some Empirical Results.* Dept. of Statistics, Berkeley Report No. 10, 25 pp.

Gautier, C., 1988: Surface solar irradiance in the Central Pacific during Tropic Heat: Comparisons between in situ measurements and satellite estimates. *J. Climate,* **1**(6), 600–608.

——, R. Frouin, B. di Julio and R. Wylie, 1986: *Net solar irradiance at the ocean surface during Tropic Heat.* Rep. to the Nat. Sci. Found., Cal. Space. Inst., Scripps Inst. of Ocean.

Halpern, D., 1984: Comparison between in situ SST measurements and the NMC SST analysis in the eastern equatorial Pacific before and during the 1982–1983 El Nino. *Proc. of the Eight Annual Climate Diagnostics Workshop,* Downsview, Canada, 100–110.

Johnson, E. S., L. A. Regier and R. A. Knox, 1988: A study of geostrophy in tropical Pacific Ocean currents during the NORPAX Tahiti shuttle using a shipboard doppler acoustic current profiles. *J. Phys. Oceanogr.*, **18**, 708–723.

Katsaros, K. B., 1980: The aqueous boundary layer. *Bound.-Layer Meteor.*, **18**, 107–127.

Koblinsky, C. J., R. L. Bernstein, W. J. Schmitz and P. P. Niiler, 1984: Estimates of the geostrophic stream function in the western north Pacific from XBT surveys. *J. Geophys. Res.*, **89**, 10 451–10 460.

Kidwell, K. B., 1986: *NOAA Polar Orbiter Data Users Guide.* NOAA National Environmental Satellite, Data, and Information Service, National Climate Data Center, Satellite Data Services Division, Washington, DC.

McClain, E. P., W. G. Pichel and C. C. Walton, 1985: Comparative performance of AVHRR-based multiChannel sea surface temperature. *J. Geophys. Res.*, **90**(C6), 11 587–11 601.

NOAA/ERL, 1985: *EPOCS, Progress and Plans,* 90 pp.

Njoku, E. G., 1985: Satellite derived sea surface temperature workshop comparisons. *Bull. Amer. Met. Soc.*, **66**, 274–281.

O'Neill, M., I. G. Sinclair and F. J. Smith, 1969: Polynomial curve fitting when abscissas and ordinates are both subject to error. *Comput. J.*, **12**, 52–56.

Patzert, W. C., T. P. Barnett, M. H. Sessions and B. Kilonsky, 1978: AXBT observations of tropical Pacific Ocean thermal structure during the NORPAX Hawaii/Thaiti shuttle experiment November 1977 to February 1978. Scripps Inst. of Ocean., SIO Ref #78–24.

Pullen, P., 1985: Sea surface temperatures in the eastern equatorial Pacific from ship data report, Pac. Mar. Environ. Lab., Nat. Ocean. Atmos. Admin, Seattle, Washington.

Press, W. H., B. P. Flannery, S. A. Teukolsky and W. T. Vetterling, 1986: *Numerical Recipes.* Cambridge University Press., 818 pp.

Rao, C. K. N., L. L. Stowe, E. P. McClain and J. Sapper, 1990: Development and application of aerosol remote sensing with AVHRR data from the NOAA satellites. To Appear in *Aerosols and Climate.* (Eds. P. V. Hobbs and M. P. McCormick). A. Deepak publishing, Hampton, VA.

Reynolds, R. W., 1988: A real-time global sea surface temperature analysis. *J. Climate,* **1**, 75–86.

——, C. K. Folland and D. E. Parker, 1900: Biases in satellite-derived sea-surface temperature data. *Nature,* **341**, 728–731.

——, D. Marsico and W. Newell, 1988: Progress report for the TOGA SST data center. *Trop. Ocean-Atmos. Newsletter,* 10–12.

Saur, J. F. T., 1963: A study of the quality of sea water temperatures reported in logs of ships' weather observations. *J. Appl. Meteor.*, 417–425.

Strong, A. E., 1986: Monitoring El Nino using satellite based sea surface temperatures. *Ocean-Air Interactions,* **1**, 11–28.

——, and E. P. McClain, 1984: Improved ocean surface temperatures from space—Comparisons With Drifting Buoys. *Bull. Amer. Met. Soc.*, **65**(2), 138–142.

Tabatta, S., 1978: Comparison of observations of sea surface temperatures at Ocean Station P and NOAA buoy stations and those made by merchant ships traveling in their vicinity, in the northeast Pacific Ocean. *J. Appl. Meteor.*, **17**, 374–385.

Van Woert, M. L., 1988: Satellite derived estimates of monthly-averaged, tropical Pacific sea surface temperature for 1983, 1984 and 1985. SeaSpace Tech. Rep. Ref. #88-1, San Diego, 119 pp.

Wyrtki, K., and B. Kilonski, 1984: Mean water and current structure during the Hawaii-to-Tahiti Shuttle Experiment. *J. Phys. Oceanogr.*, **14**, 242–254.

York, D., 1966: Least-squares fitting of a straight line. *Canadian J. Phys.*, 1079–1086.